AOI987

The MICAD Research Team

Created: May 17, 2006; Updated: June 15, 2006.

Chemical name:	AOI987	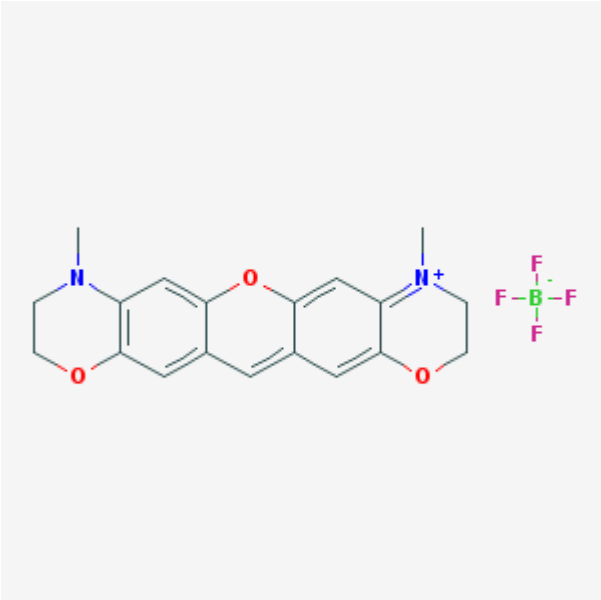
Abbreviated name:	AOI987	
Synonym:		
Agent Category:	Compound	
Target:	Aggregates of β-amyloid (Aβ) peptides	
Target Category:	Acceptor	
Method of detection:	Optical imaging (NIRF)	
Source of signal:	AOI987	
Activation:	No	
Studies:	• In vitro • Rodent	Click on the above structure for additional information in PubChem.

Background

[PubMed]

Alzheimer's disease (AD) is a major neurodegenerative disease associated with an irreversible decline of mental functions and with cognitive impairment (1, 2). It is characterized by the presence, in the brain, of senile plaques of β-amyloid (Aβ) peptides with intracellular neurofibrillary tangles of filaments containing the hyperphosphorylated protein tau (3, 4). Accelerated deposition of Aβ deposits seems to be a key risk factor associated with AD, and although the mechanisms of the disease are still not fully understood, reducing the deposition of amyloid plaques seems to benefit patients.

NLM Citation: The MICAD Research Team. AOI987. 2006 May 17 [Updated 2006 Jun 15]. In: Molecular Imaging and Contrast Agent Database (MICAD) [Internet]. Bethesda (MD): National Center for Biotechnology Information (US); 2004-2013.

Today, the clinical diagnosis of AD relies on mental and cognitive assessments of patients and the confirmation of the disease is so far obtained by postmortem examination of tissues. Major effort is being undertaken to find means of evaluating in vivo, at an early stage, the growth of the Aβ plaques for better assessment and possibly treatment.

Several radioligands for positron emission tomography (PET), such as [^{18}F]FDDNP (5), with [^{11}C]PIB (6), and [^{11}C]SB-13, have been developed and tested in humans *in vivo* (7-9). Although PET currently seems to be the most promising technique, it has several drawbacks, including the short half-lives of the positron emitting nuclei and the limited availability of the technique. Magnetic resonance imaging (MRI) does have somewhat stringent requirements on spatial resolution in order to identify individual plaques (diameter ≤ 50 μm), and while feasible on fixed human specimen using transgenic mouse models, the clinical use has not been yet possible.

Recent studies have been carried out using an alternative, all-optical, imaging technology that uses novel fluorescent amyloid dyes that absorb and emit in the near-infrared (NIR) spectrum (10-13). NIR imaging reduces the background and scattering through biological tissue usually encountered with fluorescent imaging in live animals with short wavelengths of light; it has been shown as a viable alternative for visualizing amyloid load in living mice using a fluorescent dye such as AOI987 (13). AOI987 possesses all the main characteristics needed to image Aβ plaques: 1) a low molecular weight (< 500 Da), 2) a high lipophilicity (logP 1-4, P = partition coefficient) to cross the blood-brain barrier (BBB) in sufficient amounts, 3) a fluorescence maximum within 650-900 nm.

Synthesis

[PubMed]

AOI987 can be prepared following a two-step procedure using an azo derivative as key intermediate, as described by Hintersteiner et al. (13). In this procedure, the authors prepared the azo intermediate (4-methyl-7-(4-nitro-phenylazo)-3,4-dihydro-2H-benzo[1,4]oxazin-6-ol) by dissolving 4-nitro-benzenediazonium tetrafluoroborate in 10% H_2SO_4, and subsequently adding the obtained solution to 4-methyl-3,4-dihydro-2H-benzo[1,4]oxazine-6-ol in methanol. After stirring for 30 min at 20 °C, the mixture was then neutralized with 25% aqueous ammonia, and a red precipitate containing the azo intermediate was spun down. Purification of the product was made by recrystallization in *n*-butanol. The chemical purity obtained was > 95%.

AOI987 was prepared by dissolving the azo intermediate (560 mg, 1.78 mmol) and 4-methyl-3,4-dihydro-2H-benzo[1,4]oxazin-6-ol (326 mg, 1.96 mmol) into a mixture of ethanol/water (10:1, 10 ml). After an addition of 32% HCl (700 μl), the mixture was then stirred for 1 h at 70 °C (under reflux, and finally, and was finally concentrated under reduced pressure. The obtained residue was dissolved in water and treated with a saturated solution of sodium tetrafluoroborate. The precipitate formed by this reaction

was spun down and purified using a column chromatography (SiO_2 > dichloromethane/methanol = 10:2) to produce the blue crystals of AOI987 (480 mg (1.17 mmol), 65%).

AOI987 displayed the following fluorescent properties: one single absorption maximum at 650 nm, one single emission maximum at 670 nm, a moderate absorption coefficient of 64,570 $M^{-1}cm^{-1}$, and a very high quantum yield (41%, in mouse serum) (13)

In Vitro Studies: Testing in Cells and Tissues

[PubMed]

The binding of AOI987 to amyloid plaques was assessed by incubating brain slices of female APP23 mice (average body weight ~ 25g, $3 \leq n \leq 5$) for 5 min at 20 °C with aqueous solutions of the dye, at various concentrations ranging from 0.0001% to 0.01% (wt/vol). An analysis of the tissue sections showed that the fluorescent spots co-localized with Aβ deposits stained with silver methenamine, indicating a specific staining of amyloid plaques by the oxazine dye. AOI987 showed an excellent contrast-to-noise ratio, even at very low concentrations (lowest concentration in the study was 0.0001% (wt/vol)) (13)

Differential fluorescence spectroscopy performed by Hintersteiner et al. (13) showed that the magnitude of the fluorescence shift was dependent on the concentration of aggregated Aβ peptides. The K_d value for AOI987 was estimated to be 0.2 μM. Additional studies were also performed by the authors using aggregated Aβ peptides incubated with thioflavin T to study related thioflavin T displacement. The measured fluorescence intensity showing a maximum between 460 and 560 nm (excitation 445 nm) reflected thioflavin binding to aggregated Aβ peptides. Addition of AOI987 caused a concentration-dependent reduction of the fluorescence intensity, indicating displacement of thioflavin from aggregated Aβ peptide. A calculation of the apparent binding constant for AOI987 (to aggregated A peptide) was made by measuring displacement curves, leading to values in the range of 0.1 –0.2 μM, for all thioflavin concentrations. The fact that the apparent binding constant did not increase with the thioflavin concentration showed that the displacement of thioflavin from aggregates Aβ did not occur by a simple competitive mechanism.

Animal Studies

Rodents

[PubMed]

The BBB penetration of AOI987 was assessed *ex-vivo* by Hintersteiner et al. (13), using groups of n=4 wild-type mice (C57BL/6Jico). Briefly, the experimental protocol involved injecting the dye intravenously to the animals (injection volume of 10ml/kg of tissue, using 0.9% saline as vehicle). After sacrifice of the mice at various time points (n = 4 each,

5 min to 2 h), AOI987 levels were determined in plasma and brain tissue extracts using liquid chromatography/mass spectrometry methods.

Results showed a maximal plasma concentration of AOI987 obtained within 15 min after injection. The dye was rapidly eliminated from circulation, with residual plasma levels < 10% of the initial concentration, 2 h after administration. The elimination of AOI987 from the brain compartment was slightly slower and the brain concentration of AOI987 was greater than the corresponding plasma levels at all time points measured by the authors, indicating a rapid and significant penetration of AOI987 through the intact blood-brain barrier. In this study (13), the limit of quantification reported was 3 pmol/ml plasma and 15 pmol/g brain.

In vivo NIRF imaging of Aβ using AOI987 was also reported by Hintersteiner et al. (13). The experiments were carried out with female 17-month-old APP23 transgenic mice (n = 3 to 5) and age-matched wild-type littermates (n = 2 to 4). AOI987 was injected intravenously through the tail vein at the following concentrations: 0.1 (established optimal dose), 1 and 3 mg/kg of tissue (in 0.9% saline). Results showed an intense fluorescence signal in the brain, very shortly after injection of the dye. The disappearance of the fluorescence signal was substantially slower in transgenic APP23 as compared with wild-type animals. Reported values (extracted from figures provided by the authors) of the relative fluorescence signal (in %), using the optimal dose of injected dye, were as follows: ~62 at 60 min post-injection (no significant difference between wild and APP23 mice); ~40 for wild-type mice and ~50 for APP23 mice, at 120 min post-injection ($P < 0.001$); ~40 for wild-type mice and ~25 for APP23 mice, at 240 min post-injection.

In their study, Hintersteiner et al. (13) defined 'specific binding' of AOI987 as (the fluorescence signal for transgenic mice – the fluorescence signal for wild-type mice)/the flurorescence signal for transgenic mice. The reported values for specific binding (extracted from figures), after injection of 0.1mg/kg AOI987 were as follows: ~0.25 at 60 min post-injection, ~0.4 at 120 min post-injection.

Additional NIRF-AOI987 *in vivo* studies using younger mice showed a similar signal pattern between 6-month- and 9-month-old mice, and a complementary histological analysis showed that the minimum age at which the differences between AAP23 transgenic and wild-type mice was 9 months.

Other Non-Primate Mammals

[PubMed]

No publication is currently available.

Non-Human Primates

[PubMed]

No publication is currently available.

Human Studies

[PubMed]

No publication is currently available.

References

1. Heininger K. A unifying hypothesis of Alzheimer's disease. IV. Causation and sequence of events. Rev Neurosci, 11 Spec No: p. 213-328. 2000.
2. Forstl H, Kurz A. Clinical features of Alzheimer's disease. Eur Arch Psychiatry Clin Neurosci. 1999;249(6):288–290. PubMed PMID: 10653284.
3. Hardy J. The relationship between amyloid and tau. J Mol Neurosci. 2003;20(2):203–206. PubMed PMID: 12794314.
4. Brandt R, Leschik J. Functional interactions of tau and their relevance for Alzheimer's disease. Curr Alzheimer Res. 2004;1(4):255–269. PubMed PMID: 15975055.
5. Shoghi-Jadid K, Small GW, Agdeppa ED, Kepe V, Ercoli LM, Siddarth P, Read S, Satyamurthy N, Petric A, Huang SC, Barrio JR. Localization of neurofibrillary tangles and beta-amyloid plaques in the brains of living patients with Alzheimer disease. Am J Geriatr Psychiatry. 2002;10(1):24–35. PubMed PMID: 11790632.
6. Klunk WE, Engler H, Nordberg A, Wang Y, Blomqvist G, Holt DP, Bergstrom M, Savitcheva I, Huang GF, Estrada S, Ausen B, Debnath ML, Barletta J, Price JC, Sandell J, Lopresti BJ, Wall A, Koivisto P, Antoni G, Mathis CA, Langstrom B. Imaging brain amyloid in Alzheimer's disease with Pittsburgh Compound-B. Ann Neurol. 2004;55(3):306–319. PubMed PMID: 14991808.
7. Nordberg A. PET imaging of amyloid in Alzheimer's disease. Lancet Neurol. 2004;3(9):519–527. PubMed PMID: 15324720.
8. Bacskai BJ, Hickey GA, Skoch J, Kajdasz ST, Wang Y, Huang GF, Mathis CA, Klunk WE, Hyman BT. Four-dimensional multiphoton imaging of brain entry, amyloid binding, and clearance of an amyloid-beta ligand in transgenic mice. Proc Natl Acad Sci U S A. 2003;100(21):12462–12467. PubMed PMID: 14517353.
9. Wu C, Pike VW, Wang Y. Amyloid imaging: from benchtop to bedside. Curr Top Dev Biol. 2005;70:171–213. PubMed PMID: 16338342.
10. Nesterov EE, Skoch J, Hyman BT, Klunk WE, Bacskai BJ, Swager TM. In vivo optical imaging of amyloid aggregates in brain: design of fluorescent markers. Angew Chem Int Ed Engl. 2005;44(34):5452–5456. PubMed PMID: 16059955.
11. Skoch J, Dunn A, Hyman BT, Bacskai BJ. Development of an optical approach for noninvasive imaging of Alzheimer's disease pathology. J Biomed Opt. 2005;10(1): 11007. PubMed PMID: 15847573.
12. Frangioni JV. Self-illuminating quantum dots light the way. Nat Biotechnol. 2006;24(3):326–328. PubMed PMID: 16525407.
13. Hintersteiner M, Enz A, Frey P, Jaton AL, Kinzy W, Kneuer R, Neumann U, Rudin M, Staufenbiel M, Stoeckli M, Wiederhold KH, Gremlich HU. In vivo detection of amyloid-beta deposits by near-infrared imaging using an oxazine-derivative probe. Nat Biotechnol. 2005;23(5):577–583. PubMed PMID: 15834405.